

## Mapping the Optically-Aberrating Environment in a Partially-Quieted Mach 0.6 Free Shear Layer

John P. Siegenthaler\*, Stanislav Gordeyev\*\*  
and Eric J. Jumper†

*Center for Flow Physics and Control*  
Department of Aerospace and Mechanical Engineering  
The Hessert Laboratory  
University of Notre Dame  
Notre Dame, Indiana 46556

### Abstract

This paper reports on our progress toward regularizing the coherent, vortical structures in a planar, high-Mach-number, subsonic free shear layer. The purpose of regularizing the structures is to reduce the bandwidth required by an adaptive optic system to correct for the aero-optic aberrations imposed on a laser beam passing through the shear layer. It is well known that forcing shear layers in the high-Mach subsonic regime in order to regularize (i.e., make periodic) the formation of structures is difficult because of all the sources of excitation at these flow conditions. The present effort was to examine the forcing environment remaining after attempting to suppress the influence of compressor noise by inserting a sonic throat downstream of the test section. Optical characterization of the “quieted” shear layer propagation environment demonstrated that the layer was receptive to the remaining vibration excitations, which dominated the formation of structures over the 50 cm window examined. This paper draws a number of important conclusions relevant to the problem of regularizing shear layers in this Mach number regime.

### Introduction

When an otherwise-planar, optical wavefront is made to propagate through a variable-index-of-refraction, relatively-thin, turbulent flow, the wavefront becomes aberrated. The study of the effect of optical propagation through such flow fields is referred to as aero-optics.<sup>1,2</sup> The rapidly-time-varying aberrations imposed on the wavefront degrade the performance of an optical system

attempting to make use of the optical signal. Variable-index turbulent flow fields may have their origin in the mixing layer between two dissimilar-index flow streams (two-index mixing),<sup>3,4</sup> or may be caused by projecting the optical beam through high-Mach, boundary and free shear layers. The latter scenario is relevant to the use of airborne lasers with flight Mach numbers greater than 0.6.<sup>5-7</sup> For free shear layers at these Mach numbers, with convective Mach numbers of 0.45 and less, the associated flow fields are generally considered “incompressible”; yet, it is well known that laser propagation through such layers greatly affects the beam quality (wavefront figure) of a laser propagated through them.

In three previous papers,<sup>8,9,10</sup> we presented data on the dynamic optical distortion imposed on an otherwise planar wavefront made to propagate through an unforced free shear layer with ranges in Mach number from 0.73 to 1.09 on the high-speed side and Mach 0.1 to 0.2 on the low-speed side. These data were collected in a shear layer facility at the Arnold Engineering Development Center (AEDC) and in the Weakly-Compressible Shear Layer (WCSL) facility in the Hessert Laboratory at Notre Dame. The shear layers corresponded to Reynolds numbers for the high- and low-speed streams of  $12-14 \times 10^6 \text{ m}^{-1}$  and  $1.4-3.0 \times 10^6 \text{ m}^{-1}$ , respectively.

A model for the index field was developed, the “Weakly-Compressible Model” (WCM)<sup>11</sup>, to explain the aberrating effect of a free shear layer in this Mach number range. The cornerstone of the model is that the variation in index of refraction through the shear layer is due primarily to static pressure fluctuations concomitant with the high flow curvature associated with the organized vortical structures in the shear. The pressure field is related to a drop in the density field, which is, in turn, directly related to a change in the air’s index of refraction.

In two previous papers, we presented results from a test series performed in the WCSL facility; these papers presented experimental verification of both the presence of pressure wells associated with the coherent

---

\*Graduate Research Assistant

\*\*Assistant Research Professor, Member AIAA.

†Professor, Fellow AIAA

Copyright ©2003 by J.P. Siegenthaler, S. Gordeyev and E.J. Jumper,  
Published by the American Institute of Aeronautics and Astronautics,  
Inc. with permission.

structures in the layer that corresponded to those predicted by the Weakly Compressible Model (WCM)<sup>12</sup> and aberrated wavefronts that also corresponded to those predicted by the WCM<sup>10</sup>. It should also be noted that, for the case of the Mach 1.09 shear layer, while the aberrations are irregular, they repeat at a center frequency of approximately 1.1 kHz; these are the "naturally-occurring" aberrations in the unforced shear layer. Figure 1 is taken from Ref.<sup>12</sup> showing one of the coherent structures responsible for the Optical aberrations.

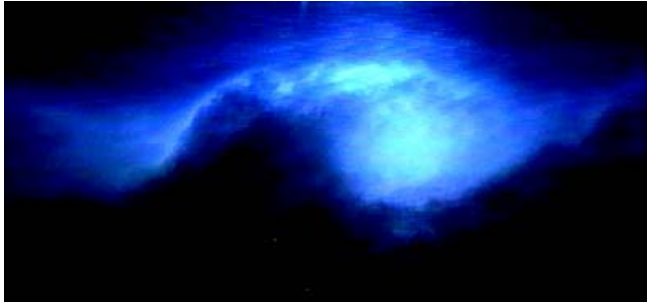


**Figure 1. Flow Vapor Visualization of a Coherent Structure in a Mach 1.09 Shear Layer from 50 – 65 cm downstream of the splitter plate in the Notre Dame Weakly-Compressible Shear Layer Facility<sup>12</sup>.**

**Motivation for the Present Effort**

Based on the wavefront data collected at both the AEDC facility and the Notre Dame WCSL facility, two things are immediately apparent: first, the aberrations over a 20 cm aperture yield peak-to-peak OPD as high as 5 μm; second, an adaptive optic (AO) system, consisting of wavefront sensor, reconstructor, associated electronics and deformable mirror (DM) would require a bandwidth of at least 10 kHz to correct these aberrations. At this time, the limiting function of an AO system would be the ability to construct real-time, streaming conjugate wavefronts to the DM’s electronic driver with no time delay. Work reported in Refs.<sup>13,14</sup> for a 7 m/s heated jet, suggested that locking the coherent structures to a forcing signal (“regularizing” the structures) could reduce the bandwidth requirements for an AO system. In those studies the heated jet was forced using a speaker located at approximately 2 m from the jet exit nozzle. In the heated-jet case, the shear-layer roll up was controlled by forcing the layer at 239 Hz. This frequency was approximately the most unstable frequency in the shear layer, based on the measured feeding-boundary-layer thickness and the relationship between frequency and momentum thickness in a feeding layer as given in Ho and Huerre<sup>15</sup> as

$$\frac{f\theta}{U_c} \cong 0.032 \tag{1}$$

where  $f$  is the most amplified frequency,  $\theta$  is the momentum thickness,  $U_c$  is the convective speed (phase velocity) and the value 0.032 is the maximum point on the curve of data for the amplification rates based on Ho and Huerre’s<sup>15</sup> Fig. 2(a). It should be noted that while this the most-amplified frequencies, there is a broad range of frequencies that have only slightly-less amplification centered at the Eq. (1) frequency.

The suggestion of Ref.<sup>14</sup> was to force the weakly-compressible free shear layer; however, forcing of a high-Mach, subsonic shear layer is not as easy as forcing a low Mach number shear layer like that used in the heat-jet experiments. To our knowledge, successful forcing of this high a Reynolds number layer has not yet been reported. The problem we face is doubly difficult if our attempt is to regularize the coherent structure at 0.5 m, since, as can be seen in Fig. 1, by 0.5 m down stream from the splitter plate, there is evidence in the visualization that a number of pairings have taken place.

In our last paper on this topic<sup>16</sup>, we attempted to use single-dielectric, dielectric barrier discharge plasmas, or plasma actuators<sup>17</sup> to force both the Mach 1.09 shear layer and a Mach 0.73 shear layer. The plasma actuator configuration is shown in Fig. 2. The Ref.<sup>16</sup> attempt met with some success; however, the results raised a number of questions.

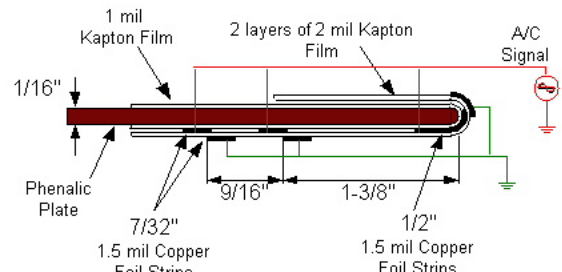


**Figure 2. Single-Dielectric, Dielectric Barrier Discharge Plasma Actuator used in the Previous Study<sup>16</sup>.**

The first attempt was to force the Mach 1.09 shear layer, at the splitter plate, at approximately the passage frequency of the coherent structures visualized using a strobe to illuminate the water vapor that condensed along the shear layer due to the low-pressure cells that form in the coherent structures (as in Fig. 1). In order to change the strobe frequency along with the forcing frequency, the strobe was triggered at a subharmonic of the forcing frequency, by building a circuit that divided the forcing frequency by 16.

The plasma was made to pulse on and off over a range of discrete frequencies around the passage frequency. The success of the forcing was qualitatively determined by how much or how little “jerkiness” was perceptible to the eye as the strobe was flashed at subharmonics of the passage frequency. The flashing of

the plasma was generated by running the shielded electrodes with an AC signal above and below ground by approximately 5 kV with a given waveform (square, sinusoidal or triangular) at a fixed frequency, ranging, depending on the run, from 5 to 8 kHz. The unshielded electrodes were also run between the same voltage levels using the same waveform, but shifted in frequency by the desired on-off forcing frequency; this caused the actuator to turn on and off at the difference or beat frequency. Because of the need for relatively-high humidity in the ambient laboratory air in order for the water vapor to condense, the tests, being in December, allowed for the visualization runs to be limited to the Mach 1.09 case and these tests were limited to only a single days efforts.

As reported in Ref.<sup>16</sup>, for whatever reason, using the strobe visualization, forcing near the passage frequency did not seem to have any beneficial effect on quieting the jerkiness of the visualized structures position. This is contrary to what we had suspected; Oster and Wynanski<sup>18</sup> reported that in a high Reynolds number free shear layer, forcing of a desired frequency caused a flattening of the growth in the momentum thickness over a relatively large streamwise range.

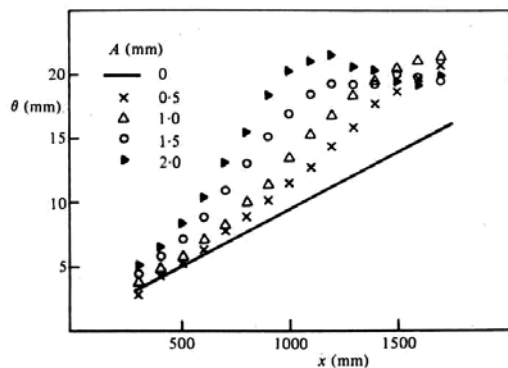


Figure 3. Effect of Amplitude of oscillation of a trailing-edge flap, 1.0 cm long, located at the trailing edge of the splitter plate, forced at 40 Hz on the shear-layer momentum thickness,  $\theta$ <sup>18</sup>.

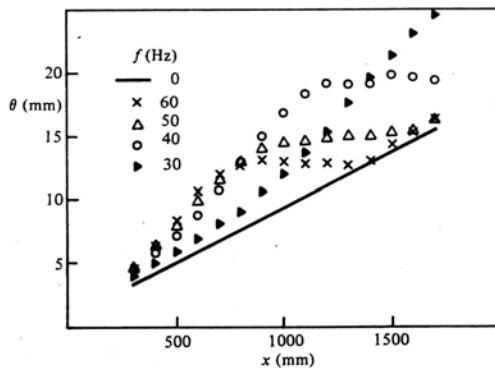


Figure 4. Effect of frequency of oscillation of a trailing-edge flap, 1.0 cm long, located at the trailing edge of the splitter plate, forced at an amplitude of 1.5 mm on the shear-layer momentum thickness,  $\theta$ <sup>18</sup>.

Based on the accompanying flow visualizations and spectra in the paper, our interpretation of their data, as in Figs. 3 and 4, suggested that relatively modest amplitudes of the forcing, consistent with the coherent two-dimensional-structure passage frequency, would affect a regularization of the structure size over some streamwise distance consistent with the extent of the flattening in Figs. 3 and 4.

As reported in Ref.<sup>16</sup>, when we broadened our range of forcing frequency, we were able to smooth the jerkiness of structures location; however, this required forcing at greater than 4 kHz. Since the strobe trigger was linked to the forcing frequency, in retrospect, it may have been that the natural structure formation was fairly regular to begin with. Rather than the plasma having any forcing effect, our adjustment of the forcing frequency may only have caused the strobe to sink up to a subharmonic of the “naturally-occurring” passage frequency. With the strobe frequency at 1/16<sup>th</sup> of the forcing frequency, the strobe frequency would have been approximately 260 Hz. Thinking in terms of a subharmonic, four times 260 Hz is very close to the passage of 1080 reported earlier in Ref.<sup>12</sup>, as measured by unsteady pressure transducers. Optical measurements made in an attempt to confirm the regularization did not appear to be any cleaner than the unforced case reported in Ref.<sup>10</sup>. On the other hand, as reported in Ref.<sup>16</sup>, we were able to show good correlation in the optical signal at a measurement location of 15 cm downstream from the splitter plate for forcing with the plasma actuator at 1.67 kHz, for example. Figure 5 is an example of the optical response to the plasma actuator being modulated to force the layer at 1.67 kHz.

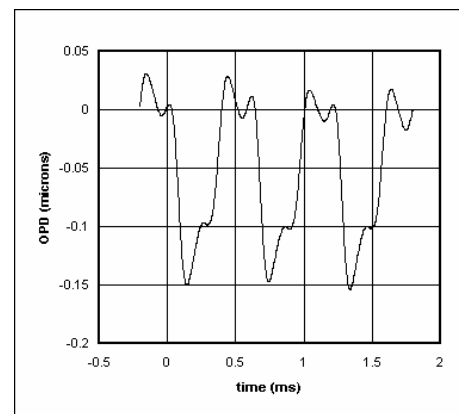


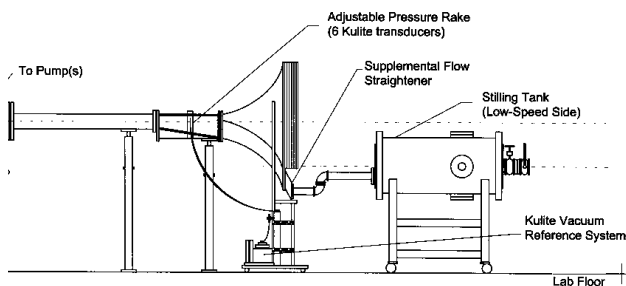
Figure 5. Forced, Phase-Lock Averaged OPD, for a Sine Wave, 1.67 kHz Forcing Frequency, Triggered off the Forcing Frequency.

These Ref.<sup>16</sup> results caused us to step back from the work and reevaluate our notions of forcing the shear layer for regularization as far as 0.5 m downstream of the splitter plate in high-Mach, subsonic shear layers. It was clear that the tunnel exposed the shear layer to many

sources of excitation, not the least of which was the acoustic and fluctuating pressure impulses coming from the vacuum pumps. Our first attempt at quieting the shear layer's environment was to design a flow-choking nozzle to prevent the pump-related noise from reaching the test section directly through the flow passage. This paper reports on the optical aberrations present in the shear layer when a sonic throat was placed downstream of the test section with mass flow such that the high-speed stream was fixed at 0.6 Mach on the high-speed side and 0.15 Mach on the low-speed side of the shear layer.

### Weakly-Compressible, Free-Shear-Layer Facility

The present aberration frequency-mapping experiments were performed in a modified version of the facility used for Ref.<sup>16</sup>, the Notre Dame Weakly-Compressible Shear Layer (WCSL) facility, which has been described in some detail elsewhere<sup>10,12</sup>. The WCSL facility consists of an inlet nozzle and test section matted with one of Notre Dame's three transonic in-draft, wind-tunnel diffusers. The diffuser section is attached to a large, gated plenum. The plenum is, in turn, connected to three Allis Chalmer 3,310 CFM vacuum pumps. Depending on the gate-valve arrangements, each of these pumps can be used to power separate diffusers, or they can be used in combination to power a single diffuser. In the present case, only one pump was used to power the free-shear-layer facility. The general arrangement of the facility, without the sonic throat in place is shown in Fig. 6. The sonic throat section was constructed and placed in the facility just downstream of the shear-layer test section and just upstream of the diffuser.



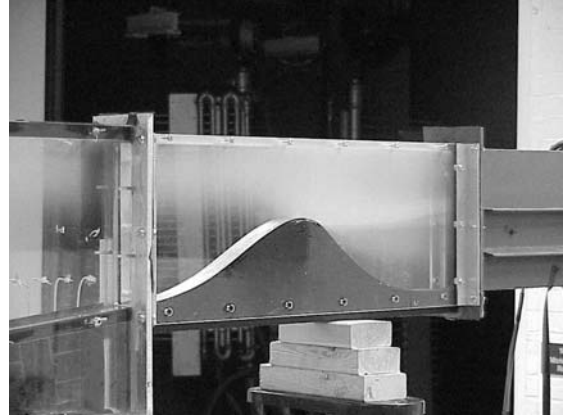
**Figure 6. Schematic of the Notre Dame High-Mach Free-Shear-Layer Facility without the sonic throat installed. Flow is from right to left.**

Figure 7 shows a photograph of the sonic throat in place downstream of the test section for the Mach 0.6 shear layer throat.

Being an in-draft tunnel, the feeding source is the room total pressure and temperature. The test section is fed from a 104-to-1 inlet nozzle directly from room total pressure on the high-speed side. On the low-speed side, room-total-pressure air is first passed through two gate

valves to lower its total pressure, while keeping its total temperature the same as the high-speed sides.

**Optical Measurements.** In the present set of experiments only a Malley Probe was used to assess the optical aberrations. The Probe is described in detail in



**Figure 7. Sonic Throat in place downstream of test section, flow is from left to right.**

Ref.<sup>19</sup>. In the present case, the Malley Probe's two laser beams were inserted into the test section from below, as shown in Fig. 8; their spacing was 4.5 mm apart, aligned in the streamwise direction. As described in Ref.<sup>19</sup>, the second beam was used to extract group or convective velocity data contained on the beam-deflection angles using the spectral method.

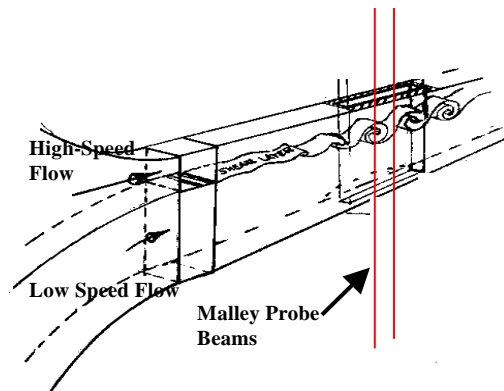


**Figure 8. Close-up Schematic of the Test Section.**

Knowing the displacement between the beams, the convective velocity could be computed. As described in Reference<sup>20</sup>, the deflection angle of the probe beam is the spatial derivative of a wavefront for a larger-aperture, otherwise planar wavefront that would be present if that wavefront were aberrated by the same flow. The fact that the aberrations "convect" with the convecting fluid structures causing the aberrations makes it possible to infer the aberrated OPD as a function of time; this fact was first proposed by Malley et. al.<sup>21</sup> The Malley probe

was set up on an optical bench below the WCSL test section, as shown in Fig. 9. The probe beams were directed up normal to the shear layer, into the tunnel, through the



Figure 9. WCSL Facility with Malley-Probe Set Up on the Optical Bench.

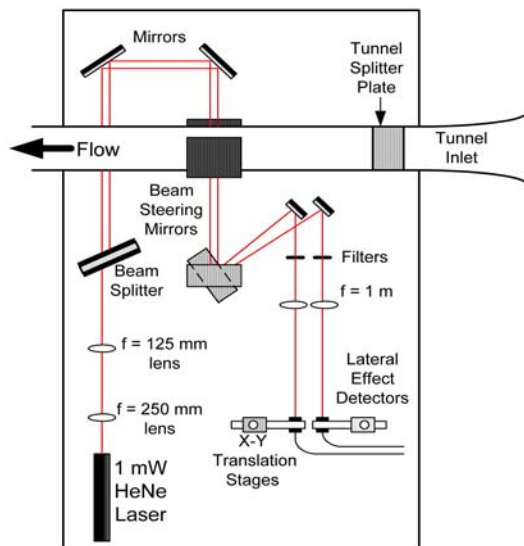


Figure 10. Plan-View Schematic of the Optical Bench. Data Acquisition

shear layer, and out of the tunnel. Once out of the tunnel, the beams were reflected off two steering mirrors back onto the optical bench. The beams were then directed to Lateral Effect detectors, where their deflections (beam jitters) were measured. This is shown schematically in Fig. 10.

**Results**

**Flow Conditions.** As mentioned earlier, with the sonic throat in place, the tests were run at a single flow condition of Mach 0.6 on the high-speed side and Mach

0.16 on the low speed side. Static pressure measurements were made along the wall of the test section and showed that with the sonic throat in place, the test section had nearly constant pressure, with only a slightly favorable pressure gradient. Figure 11 shows the pressure drop along the test section.

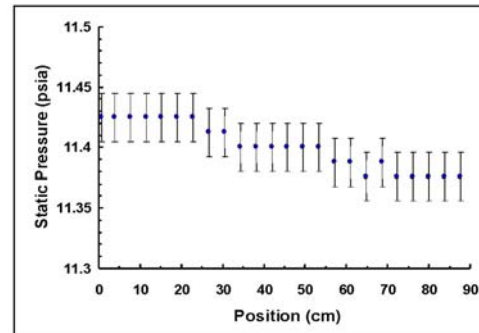


Figure 11. Static Pressure along the Test Section.

Although detailed feeder boundary-layer measurements were not made, sufficient measurements were made to estimate the initial momentum thickness of the shear layer,  $\theta_0$ , to be approximately 1- 1.5 mm. This thickness and Eq. (1) were used to estimate of the initial most-unstable initial frequency to be approximately 3 - 4 kHz. This gives a wavelength of approximately 3 - 4 cm, so the first rollup of the shear layer would not be expected until after 10 - 12 cm.

**Malley Probe Results.** A series of Malley probe measurements were made a various locations starting at 1.4 cm downstream from the splitter plate out to 49 cm from the splitter plate. From 1.4 - 20 cm, these measurements were made every cm and thereafter at approximately every 2 cm. These data were in the form of time series of probe beam displacements collected at 40 kHz. In addition to these flow measurements, the optical bench was moved to a position where the probe beams traveled only through the room air near the sides of the tunnel. These latter measurements were made to collect only those jitter signals due to vibration.

**PSD Results.** Power Spectral Density (PSD) of the time series of jitter measurements were made. The PSD of the vibration-only signal is shown in Fig. 12; the flow related PSD's are plotted against measurement location from the splitter plate in Fig. 13. It is clear from Fig. 12 that there are a number of sharp vibration peaks, all at frequencies less than approximately 1.5 kHz. Figure 13(a) shows that the canonical decrease in frequency with position along the shear layer is present in the PSD.

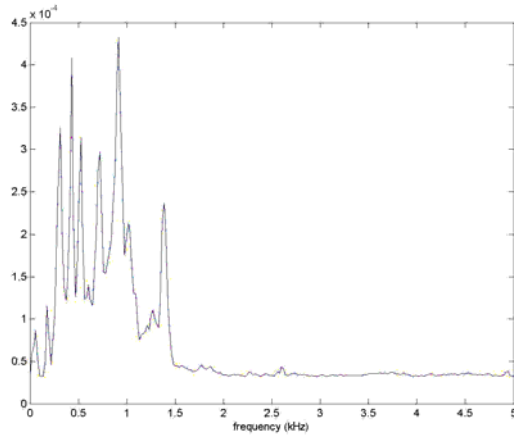
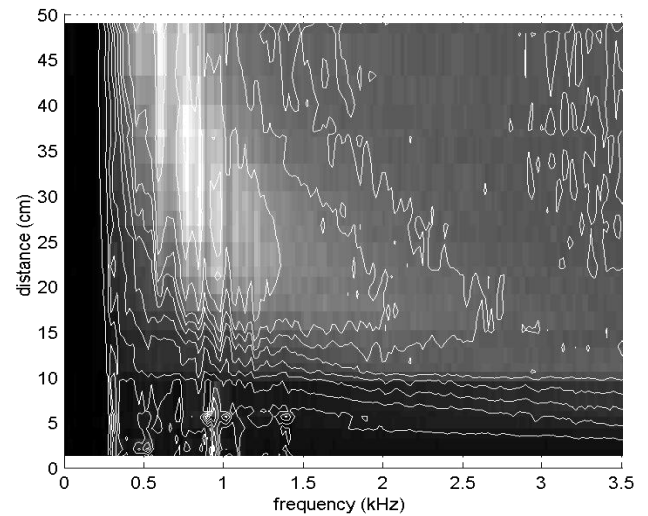


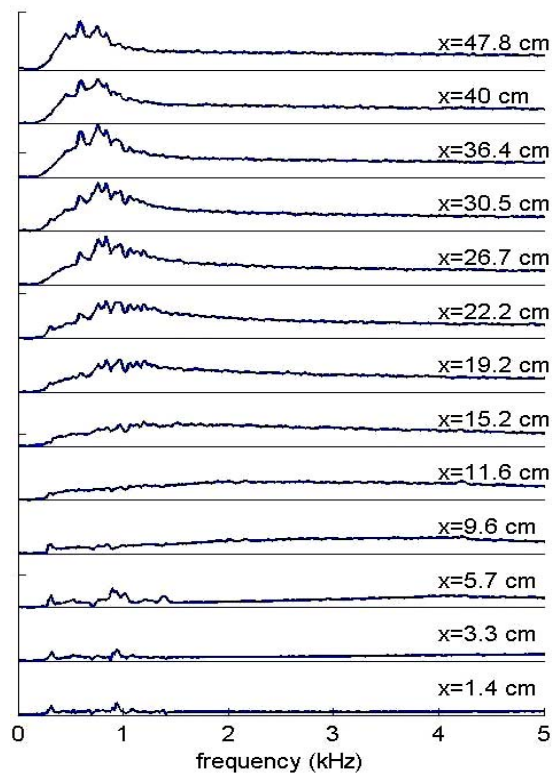
Figure 12. PSD of Vibration-Only Jitter Data.

There is also a clear rise in the intensity of the signal at positions greater than approximately 12 cm from the splitter plate. As described in Ref.<sup>11</sup>, the largest source of aberration in the shear layer is the formation of coherent structures. Referring to the last section, the increase in PSD after 12 cm is consistent with the onset of rollup in the shear layer that should begin at approximately this location. Although the intensity of the signal is considerably lower, it is clear that prior to 12 cm there are still convecting jitter signals at frequencies greater than approximately 3.5 kHz. In Refs.<sup>8,9</sup> these higher frequency aberrations were hypothesized to be due to the turbulent boundary layer, either being fed into the shear layer at the splitter plate or along the wall on the high-speed side of the layer at the location where the probe beam passes out of the tunnel. As will be shown below, this latter explanation is compatible with the velocity information extracted from the data; this will be discussed in the next section.

For the lower-frequency aberrations starting at approximately 12 cm there are clear, relatively-narrow bands of frequencies that begin at some specific distance from the splitter plate, amplify with increasing distance and then die off. The lower the frequency band the more delayed in position they begin, amplify and die off. These coherent-structure aberrations are clearly not associated with period doubling, but rather are at what appear to be unrelated frequencies. There is, however, a very clear relationship between these frequencies and the vibration frequencies shown in Fig. 12. Figure 14 shows a single-location PSD with a direct comparison to the vibration spectra for location  $x = 43.2$  cm.



(a)



(b)

Figure 13. PSD of Flow-Induced Jitter versus Location from Edge of Splitter Plate, (a) Contour Plot, (b) Individual PSD's.

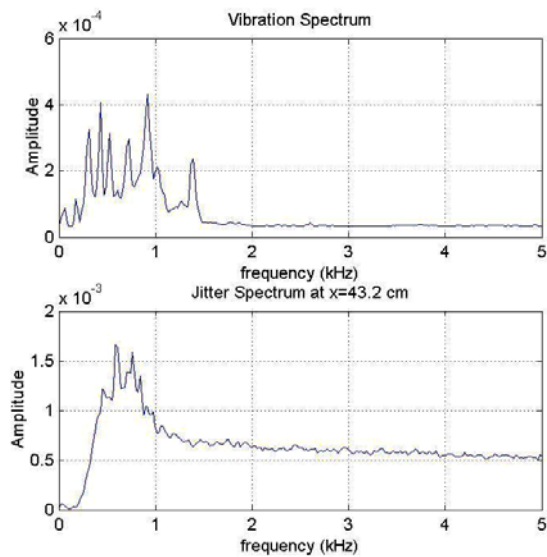


**Figure 14. Comparison of Frequencies Present in the Shear Layer and Those in the Vibration Spectra.**

The influence of the vibration on the formation of structures of a specific size is probably most-clearly demonstrated in Fig. 13(a) for the frequencies centered at 890 Hz. Although relatively low amplitude, it is clear that that a peak at 890 Hz is present in the PSD at locations less than 10 cm; at these positions, the weak peak in the PSD at 890 Hz is due to vibration induced jitter on the optical bench. On the other hand, once the shear layer has widened an extent that it is receptive to amplification of this frequency (i.e., for  $x > 20$  cm) that frequency begins to appear in the convected shear-layer aberrations. Although lower in amplitude, similar comparisons can be made with the less-than-10 cm spectra and the major peaks in the spectra of the shear layer at distances greater than 20 cm from the splitter plate.

**Aberration-Velocity Results.** The spectral method described in Ref.<sup>19</sup> was used to extract the aberration convection velocities from the jitter-signal time series. Prior to this study, a single, “average” convection velocity was always calculated for all frequencies taken together; however, in the present study a number of extracted velocities were larger than would be expected for aberrating flow structures that would be convecting in the shear layer. The velocity data near the splitter plate were particularly instructive, because across the frequency domain, the convection velocity fell comfortably on a linear fit through the phase versus frequency diagram, as in Fig. 15(a), at  $x = 9.6$  cm. As mentioned earlier, no coherent structure formation would be expected in the shear layer at this location. The reader is referred to Ref.<sup>19</sup> for details; however, the slope of the linear fit is directly related to the velocity, with the

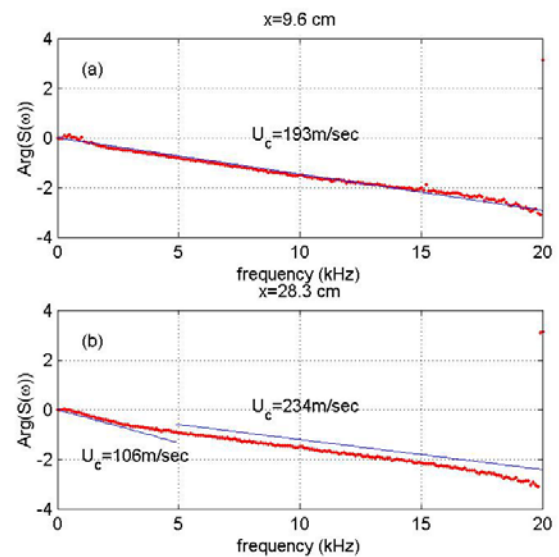


**Figure 15. Velocity trends.**

steeper the slope suggesting slower velocities. The Fig. 15(a) data give a convection velocity close to the velocity of the high-speed flow at that location, consistent with the findings of Ref.<sup>19</sup> for an attached turbulent boundary layer. On the other hand, further downstream where coherent structures are clearly formed in the shear layer, there appears to be two velocity regimes separated by frequency. The lower frequencies have velocities consistent with that that would be expected for structures convecting with the shear layer; the higher convection-velocity regime is for the higher frequencies more applicable to the turbulent boundary layer along the upper test-section wall. This lends credibility to the interpretations of Refs.<sup>8,9</sup> that the higher-frequency aberrations being associated with the turbulent boundary layer; however, now it is clear that they are due to the boundary layer on the top of the tunnel and not remnants of the turbulent boundary layer structures fed into the shear layer at the splitter plate.

After coherent structures have formed in the shear layer, there is a clear split in the velocity fits for the lower-frequency, shear-layer-convected structures and the higher-frequency structures associated with the attached turbulent boundary layer, as can be seen in Fig. 15(b). The shear-layer structures convect with the expected shear-layer convection velocity, while the boundary layers convect at higher velocity. Having the ability to robustly extract velocity data from the jitter signals also revealed an interesting trend in the velocities of the turbulent boundary layer structures (and thus the trend in the high-speed side of the shear layer); the upper, high-speed flow appears to be accelerating with increasing distance down the test section. Yet, the static pressure data, as shown in Fig. 11, would not suggest this much

acceleration if the flow were isentropic. It is clear that the flow is not isentropic, and we believe that this acceleration of the flow is probably due to the growth in the boundary layer on all sides of the tunnel. On the other hand, computing the convection velocities over the lower-frequency band shows a precipitous drop in the aberration convection velocity after about 20 cm, leveling off at the expected shear-layer convection velocity by about 30 cm. This is shown in Fig. 16.

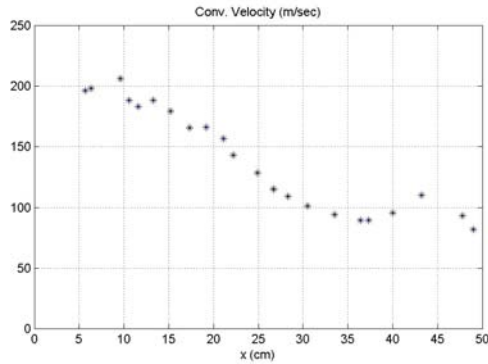


**Figure 16. Aberration Convection Velocity and Growth in  $OPD_{rms}$ .**

**Optical-Path-Difference Results.** As described in Ref.<sup>19</sup>, the jitter data and the velocity data can be combined to produce Optical Path Length as a function of time and from this Optical Path Difference (OPD) as a function of time. Then, position and time can be exchanged to produce OPD as a function of pseudo distance, as shown in Figs. 17 and 18 for two locations at  $x = 4$  cm, and  $x = 24.9$  cm. These figures contain OPD's constructed from the two beams and it can be seen that the OPD are shifted by about 5 mm, consistent with the probe beam spacing. It can also be seen that the OPD's at 4 cm have smaller spatial scale than those at 24.9 cm, consistent with the growth in the structure sizes in the shear layer. The growth in the structure sizes shows a concomitant growth in the peak-to-peak OPD consistent with that which would be predicted by the Weakly-Compressible model<sup>11</sup>.

**Discussion and Conclusions**

The purpose of this experimental series was to examine the formation of aberrating shear-layer structures in the Notre Dame WCSL facility in an attempt to understand our earlier frustrations in attempting to regularize these structures near 0.5 m downstream from the splitter plate. The suspicion prior to this series was that compressor noise propagating upstream through the diffuser and into the test section provided excitations difficult to overcome with the forcing being attempted using plasma actuators. To remove this direct path for exciting the shear layer, a sonic throat was placed between the diffuser and the test

section. The sonic throat noticeably reduced the audible noise in the facility; however, the optical aberrations due to the coherent structures present in the shear layer still

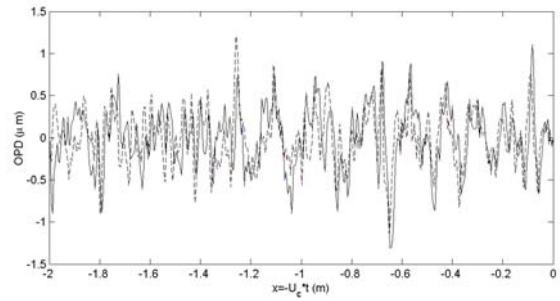


**Figure 17. OPD versus Pseudo Distance at  $x = 4$  cm.**

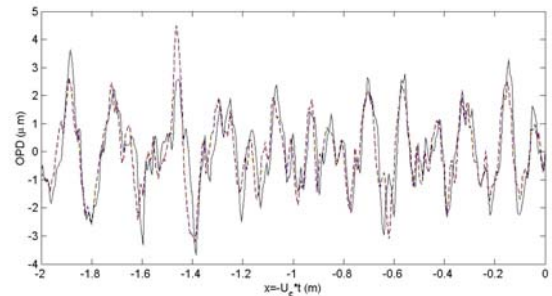


**Figure 18. OPD versus Pseudo Distance at  $x = 24.9$  cm.**

showed clear signs of responding to some source of excitation, even though in this series no deliberate excitation was being used. Comparisons between the frequencies present in the shear layer and those contained in vibration-only jitter measurements suggested that the source of the forcing was the vibration environment present in the facility.

The fact that the shear layer was receptive to these vibrations was actually a good result with respect to the original intent of regularizing the shear layer. It is now clear that high-Mach subsonic shear layers are as receptive to forcing “organized” coherent structures with relatively-low amplitude excitations, as the lower-Mach-number shear layers reported in the literature. Once formed, the structures appeared to persist for as much as 20 to 25 cm, which is also good news. On the other hand, it is clear that we must take more extensive measures to quiet the tunnel than just incorporating a sonic throat. Some obvious things that will be attempted in the near future include adding an isolation collar between the diffuser and the sonic-throat section, using vibration-isolation legs on both the inlet and test-section supports, and lining the stilling chamber with an anechoic liner. In addition, vibration-isolation legs will be added to the optical bench, although this will affect only the optical measurements themselves.



These tests also suggest a reason why the plasma actuator was able to imprint an optical-aberration onto the shear layer out to 15 cm from the splitter plate in earlier experiments, but was not able to affect the optical behavior of the shear layer further down stream. The aberration-dominating coherent structures did not form until downstream of the 15 cm location and after that the high-frequency excitation had essentially no effect on the development of the lower-frequency coherent structures. Rather, these lower-frequency structures were being driven by the other sources of excitation, including the vibration environment reported on here, but also, perhaps, by compressor noise that may have been affecting the layer in the absence of the sonic throat.

Finally, this work showed that the spectral method of determining the aberration convection velocity is sufficiently robust to be able to distinguish the differing velocities for sources of aberration that are convecting at different velocities as long as their associated frequencies are sufficiently disparate.

#### Acknowledgement

These efforts were sponsored by the Air Force Office of Scientific Research, Air Force Material Command, USAF, under Grant Number F49620-03-1-0019. The U.S. Government is authorized to reproduce and distribute reprints for governmental purposes notwithstanding any copyright notation thereon.

#### References

- [1] Gilbert, K.G., "Overview of Aero-Optics," *Aero-Optical Phenomena*, Eds. K.G. Gilbert and L.J. Otten, Vol. 80, *Progress in Astronautics and Aeronautics*, AIAA, New York, 1982, pp. 1-9.
- [2] Jumper, E.J., and E.J. Fitzgerald, "Recent Advances in Aero-Optics," *Progress in Aerospace Sciences*, **37**, 2001, pp.299-339.
- [3] Hugo, R.J. and E.J. Jumper, "Applicability of the Aero-Optic Linking Equation to a Highly Coherent, Transitional Shear Layer," *Applied Optics*, **39** (24), August 2000, pp. 4392-4401.
- [4] Cicchiello, J.M., and E.J. Jumper, "Far-Field Optical Degradation due to Near-Field Transmission Through a Turbulent Heated Jet," *Applied Optics*, **36** (25), pp. 6441-6452, September 1997.
- [5] Gilbert, K.G., "KC-135 Aero-Optical Boundary-Layer/Shear-Layer Experiments," *Aero-Optical Phenomena*, Eds. K.G. Gilbert and L.J. Otten, Vol. 80, *Progress in Astronautics and Aeronautics*, AIAA, New York, 1982, pp. 306-324.
- [6] Masson, B., J. Wissler, and L. McMackin, "Aero-Optical Study of a NC-135 Fuselage Boundary Layer," AIAA Paper 94-0277, January 1994.
- [7] Craig, J.E., J.D. Trolinger, and W.C. Rose, "Propagation Diagnostic Technique for Turbulent Transonic Flow," AIAA Paper 84-0104, January 1984.
- [8] Hugo, R.J., E.J. Jumper, G. Havener, and S.A. Stepanek, "Time-Resolved Wavefront Measurements through a Compressible Free Shear Layer," *AIAA Journal*, **35** (4), April 1997, pp. 671-677.
- [9] Fitzgerald, E.J. and E.J. Jumper, "Aperture Effects on the Aero-Optical Distortions Produced by a Compressible Shear Layer," *AIAA Journal*, 2002 (also in AIAA Paper 2000-0991, January, 2000).
- [10] Fitzgerald, E.J., Cicchiello, J.M., Siegenthaler, J.P. and Jumper, E.J., "Optical Characterization of the Notre Dame Compressible Shear-Layer Facility," AIAA Paper 02-2274, May 2002.
- [11] Fitzgerald, E.J. and E.J. Jumper, "Further Consideration of Compressibility Effects on Shear-Layer Optical Distortion," AIAA Paper 99-3617, June 1999.
- [12] Chouinard, M. Asghar, A., Kirk, J.F., Siegenthaler, J.P. and Jumper, E.J., "An Experimental Verification of the Weakly-Compressible Model," AIAA Paper 02-0352, January 2002.
- [13] Hugo, R.J. and Jumper, E.J., "Applicability of the Aero-Optic Linking Equation to a Highly Coherent, Transitional Shear Layer," *Applied Optics*, **39** (24), August 2000, pp. 4392-4401.

- [14]Cicchello, J.M. and Jumper, E.J., "Addressing the Oblique-Viewing Aero-Optic Problem with Reduced-Order Methods," AIAA Paper 2001-2799, June 2001.
- [15]Ho, C-M, and Huerre, P., "Perturbed Free Shear Layers," *Annual Reviews of Fluid Mechanics*, **16**, 1984, pp. 365-424.
- [16]Siegenthaler, J.P., Jumper, E.J., and Asghar, A., "A Preliminary Study in Regularizing the Coherent Structures in a Planar, Weakly-Compressible, Free Shear Layer," AIAA Paper 2003-0680.
- [17] Enloe, C.L., McLaughlin, T.E., VanDyken, R.D., Kachner, K.D., Jumper, E.J. and Corke, T.C., "Mechanisms and Responses of a Single Dielectric Barrier Plasma," AIAA Paper 03-1021, January 2003.
- [18] Oster, D. and Wagnanski, I, "The Forced Mixing Layer Between Parallel Streams," *J of Fluid Mechanics*, **123**, 1982, pp. 91-130.
- [19] Gordeyev, S., Jumper, E.J., Ng, T.T, and Cain, B, "Aero-Optical Characteristics of Compressible, Subsonic Turbulent Boundary Layers, AIAA Paper 2003-3606, June 2003.
- [20]Jumper, E.J. and R.J. Hugo, "Quantification of Aero-Optical Phase Distortion Using the Small-Aperture Beam Technique," *AIAA Journal*, **33**(11), 1995, pp. 2151-2157.
- [21] Malley, M, Sutton, F.W. and Kicheloe, N, "Beam-Jitter Measurements of Turbulent Aero-Optical Path Differences," *Applied Optics*, **31**, 1992, pp. 4440-4443.